Lithuanian Journal of Physics, Vol. **49**, No. 4, pp. 403–413 (2009) doi:10.3952/lithjphys.49405

AB INITIO CALCULATIONS OF CRYSTAL-FIELD FOR ACTINIDE DIOXIDES

G. Gaigalas [a], E. Gaidamauskas [a], Z. Rudzikas [a], N. Magnani [b], and R. Caciuffo [b]

[a] *Vilnius University Research Institute of Theoretical Physics and Astronomy, A. Goštauto 12, LT-01108, Vilnius, Lithuania*
E-mail: gaigalas@itpa.lt

[b] *European Commission, Joint Research Centre, Institute for Transuranium Elements, Postfach 2340, D-76125 Karlsruhe, Germany*

Received 3 August 2009; revised 27 October 2009; accepted 18 December 2009

In this paper we report on large-scale multiconfiguration Dirac–Fock and relativistic configuration-interaction calculations in the framework of crystal-field theory of the actinide dioxides. In order to be able to perform such calculations the package of the relativistic atomic structure calculations GRASP2K has been extended. The correlation and relativistic effects were taken into account. Calculated crystal-field energy levels of actinide dioxides are compared with other theoretical and with experimental results based on inelastic neutron scattering measurements.

Keywords: crystal field, crystal-field splitting, multiconfiguration Dirac–Fock, uranium dioxide, neptunium dioxide, americium dioxide, plutonium dioxide

PACS: 31.15.A, 31.15.aj, 31.15.am, 31.15.V, 75.10.Dg

1. Introduction

State-of-the-art multi-configuration Dirac–Fock calculation methods developed and optimized during the last decades are an extremely powerful tool to investigate the free-ion behaviour of elements in various oxidation states [1]. We have recently shown that, despite the large computational size of the problem, these methods can be successfully applied to describe the energy spectra of actinide ions such as americium and curium [2], the latter being up to now the heaviest element stable enough to perform extensive physical investigations on massive samples. The aim of the present work is to investigate the possible extension of such model to calculating the crystal-field (CF) energy levels *ab initio*, instead of using the simplified treatment based on the Stevens' operator-equivalent method, still treating the external ions (ligands) as point charges at fixed positions [3]. The atomic state functions are generated from very accurate atomic structure calculations in large-scale multiconfiguration Dirac–Fock approximation, including the main correlation and relativistic effects.

As a benchmark for the newly developed software we have chosen to use actinide dioxides (AnO_2), large-gap semiconductors crystallizing in the fcc fluorite structure, with $Fm\bar{3}m$ space group and relatively similar room temperature lattice parameter a_{An} ($a_{\mathrm{U}} = 5.47$ Å, $a_{\mathrm{Np}} = 5.44$ Å, $a_{\mathrm{Pu}} = 5.40$ Å, $a_{\mathrm{Am}} = 5.37$ Å, $a_{\mathrm{Cm}} = 5.36$ Å, $a_{\mathrm{Bk}} = 5.33$ Å, $a_{\mathrm{Cf}} = 5.31$ Å). The band structure comprises an occupied valence band mainly derived from oxygen 2p orbitals and an empty conduction band derived from actinide 6d and 7s orbitals, with the 5f states lying in the band gap. The occupation n of the 5f shell in the An^{4+} ion increases from 2 to 4, passing from U to Pu. In the LS coupling scheme, this corresponds to $^2\mathrm{F}_{5/2}$ ($n = 1$), $^3\mathrm{H}_4$ ($n = 2$), $^4\mathrm{I}_{9/2}$ ($n = 3$), and $^5\mathrm{I}_4$ ($n = 4$) ground multiplets. Since the 5f states are well localized the CF potential plays a central role, so that the knowledge of its size is necessary to understand both bulk and spectroscopic properties.

This family of compounds provides several model systems where the delicate balance of various interactions has been thoroughly studied [4]. The low-temperature physical behaviour of these systems is governed by a subtle interplay between CF, magneto-elastic interactions, phonon-transmitted quadrupolar interactions, and multipolar super-exchange, giving rise to a number of effects that have attracted considerable attention during the past 50 years. A crucial role is played by the CF potential acting on the actinide ions, as this quantity determines the nature of the ground state and in particular the expectation value and the polarizabil-

ISSN 1648-8504

ity of the unquenched multipolar degrees of freedom. For instance, whereas in uranium dioxide a concomitant magnetic-dipole and electric-quadrupole order has been observed [5], in neptunium dioxide the primary order parameter driving the phase transition occurring at low temperature is a rank-5 magnetic multipole [6, 7].

This work is based on the weak crystal field approximation. In this approximation crystal field was treated as the perturbation to the free-ion interactions. For the rare earth ions with two – weak crystal field affected d and medium crystal field affected f – open shells an intermediate crystal field approximation must be used. In this approximation for the ion states a basis functions of the irreducible representations of the point symmetry group were used [8].

2. Theoretical background

In the multiconfiguration Dirac–Fock method (MCDF) the atomic state function (ASF) $\Psi(\gamma PJM_J)$ of the stationary state of an atom (ion) is expressed as a linear combination of the symmetry-adapted configuration state functions (CSFs) $\Phi(\gamma_r PJM_J)$, i. e.

$$\Psi\left(\gamma PJM_J\right) = \sum_{r=1}^{m} c_r \, \Phi\left(\gamma_r PJM_J\right) . \qquad (1)$$

The mixing coefficients c_r and the one-electron radial wave functions of the Φ have been obtained with a self-consistent procedure by optimization of the energy functional based on the Dirac–Coulomb Hamiltonian, which in a. u. is given by [1],

$$H_{\rm DC} = \sum_{i=1}^{N} [c\vec{\alpha}_i\vec{p}_i + (\beta_i - 1)c^2 + V(r_i)] + \sum_{i<k} \frac{1}{r_{ik}} , \quad (2)$$

where $V(r_i)$ is the monopole part of the electron–nucleus interaction. In all calculations, the nuclear charge distribution was modelled by the two-component Fermi function.

The multiconfiguration Dirac–Fock method captures correlation effects. The relativistic configuration interaction (RCI) method can be also used to include the transverse Breit interaction at the low-frequency limit, together with self-energy and vacuum polarization QED corrections: (MCDF+B+QED). The relativistic ASF can be transformed from the jj coupling to the LS coupling using the transformation matrices [1]:

$$c_i = \sum_r b_r \left(\phi_i|\psi_r\right) . \qquad (3)$$

Here c_i is the weight of the CSF in jj coupling (see (1)), b_r is the weight in LS coupling, and $(\phi_i|\psi_r)$ is the corresponding transformation matrix [9].

In order to calculate the splitting of the energy levels – γJ of an ion in the solid matrix, the CF potential is included, using a fully *ab initio* method. In the AnO_2 fcc lattice the actinide ions occupy the 4a special positions with O_h point symmetry, whereas the oxygen ions at the 8c special positions ($\frac{1}{4}\frac{1}{4}\frac{1}{4}$, $\frac{3}{4}\frac{3}{4}\frac{3}{4}$) form an internal simple-cubic sublattice with edge length $a/2$. Treating the external ions as point charges at fixed positions, the crystal field operator (in a. u.) can be written:

$$H_{\rm CF} = \sum_{j=1}^{A}\sum_{i=1}^{N} \frac{Z_j}{\left|\vec{R}_j - \vec{r}_i\right|} =$$

$$\sum_{j=1}^{A}\sum_{i=1}^{N}\sum_{k=0}^{\infty}\sum_{q=-k}^{k} (-1)^q \, Z_j \sqrt{\frac{4\pi}{2k+1}}$$

$$\times \frac{r_i^k}{R_j^{k+1}} \, C_q^k\left(\theta_i,\phi_i\right) \, Y_{-q}^k\left(\theta_j,\phi_j\right) =$$

$$\sum_{j=1}^{A}\sum_{i=1}^{N}\sum_{k=0}^{\infty} Z_j \, \frac{r_i^k}{R_j^{k+1}}$$

$$\times \left(C^k\left(\theta_i,\phi_i\right) \cdot C^k\left(\theta_j,\phi_j\right)\right) . \qquad (4)$$

Here A is the number of the external ions (ligands), Z_j is the charge of the ligand and R_j, θ_j, and ϕ_j are the spherical coordinates. N is the number of electrons and $R_j > r_i$. Charges and positions of the ligands are the compound-dependent parameters introduced in the calculations. The splitting of degenerate atomic energy levels due to the CF (and the shift of the $J = 0$ energy level) is then calculated in first-order perturbation approximation by diagonalization of the $H_{\rm CF}$ operator matrix.

The matrix elements of the crystal field operator $H_{\rm CF}$ between two relativistic atomic state functions have the form

$$\left\langle \Psi\left(\gamma PJM_J\right)|H_{\rm CF}|\,\Psi\left(\alpha PJ'M_J'\right)\right\rangle =$$

$$\sum_{j=1}^{A}\sum_{k=0}^{j_a+j_b}\sum_{q=-k}^{k}\sum_{r,s}\sum_{a,b} c_r c_s \, (-1)^{J-M_J} \begin{pmatrix} J & k & J' \\ -M_J & q & M_J' \end{pmatrix}$$

$$\times\sqrt{2J+1}\, d_{ab}^k\left(r,s\right)\left[\kappa_a\|C^k\|\kappa_b\right](-1)^q \, Z_j\sqrt{4\pi}\times$$

$$\times\frac{Y^k_{-q}(\theta_j,\phi_j)}{\sqrt{2k+1}}\left[\int\limits_0^{R_j}\frac{r^k}{R_j^{k+1}}\left(P_aP_b+Q_aQ_b\right)\,\mathrm{d}r\;+\right.$$

$$\left.+\int\limits_{R_j}^{\infty}\frac{R_j^k}{r^{k+1}}\left(P_aP_b+Q_aQ_b\right)\,\mathrm{d}r\right], \qquad (5)$$

where

$$\left[\kappa_a\|C^k\|\kappa_b\right] =$$

$$(-1)^{j_a+1/2}\sqrt{2j_b+1}\begin{pmatrix} j_a & k & j_b \\ \frac{1}{2} & 0 & -\frac{1}{2}\end{pmatrix}\pi\left(l_a,l_b,k\right)\ . \qquad (6)$$

Here P_a and Q_a are the large and small components of the relativistic one-electron radial wave function, and

$$\pi\left(l_a,l_b,k\right)=\begin{cases}1 & \text{if } l_a+k+l_b \text{ even},\\ 0 & \text{otherwise.}\end{cases} \qquad (7)$$

The $d^k_{ab}(rs)$ in (6) are the spin-angular coefficients that arise from using Racah's algebra in the decomposition of the one-electron operator matrix element [10, 11]:

$$d^k_{ab}\left(r,s\right)\;=\;\sqrt{\frac{2j_a+1}{2J_r+1}}\;T^k_{rs}\left(ab\right)\;, \qquad (8)$$

where the coefficients $T^k_{rs}\left(ab\right)$ are defined in Eq. (64) of [11].

Degenerate γJ levels split due to the crystal field into a number of sub-levels ($a\;=\;1,\ldots,2J+1$):

$$\Psi_a\;=\;\sum_{i=-J}^{J}c_{ia}\Psi\left(\gamma PJ,M_J=i\right)\;. \qquad (9)$$

Using this method, the splitting of the energy levels (E_a) and the splitting weights (c_{ia}) can be obtained. Depending on the symmetry of the crystal some of the energy levels can retain certain degree of degeneracy. For example, in a cubic environment the ninefold degenerate $J=4$ multiplet splits into four sub-levels labelled by the irreducible representations of the cubic point group (Γ_1, Γ_3, Γ_4, Γ_5).

The CF interaction also mixes different atomic state functions (ASFs) – and important J-mixing effects are known to be present within the actinide series. In this case, taking into account n ASFs, instead of (9) the wave functions of CF sub-levels can be expressed as

$$\Psi_a\;=\;\sum_{i=1}^{n}c_{ia}\Psi\left(\gamma_iPJ_iM_{J_i}\right)\;. \qquad (10)$$

In order to be able to perform such calculations the package of the relativistic atomic structure calculations GRASP2K [12, 13] has been extended by including routines for the calculation of the matrix elements of the CF operators and for the diagonalization of the full atomic Hamiltonian matrix (including matrix elements between different ASFs).

3. Calculations of the crystal-field splitting of the ground state of U^{4+} ion

In the paramagnetic phase of UO_2, the ninefold degenerate $J=4$ multiplet splits into a Γ_1 singlet, a Γ_3 doublet, and two triplets, Γ_4 and Γ_5 [14, 15]. The approach described below was used to generate the CSFs (see (1)) for the free U^{4+} ions. The CSFs of the multiconfiguration calculations include single and double substitutions from the valence 5f shell (valence–valence correlation). Restricted active spaces (RAS) of the CSFs have been generated using the following active sets (ASs) of the orbitals:

$$\mathrm{AS}_{0'} = 1s^22s^22p^63s^23p^63d^{10}4s^24p^64d^{10}4f^{14}\;5s^25p^65d^{10}6s^26p^65f^2 \qquad (11)$$

(ASF with **1** CSF in jj coupling),

$$\mathrm{AS}_0 = 1s^22s^22p^63s^23p^63d^{10}4s^24p^64d^{10}4f^{14}\;5s^25p^65d^{10}6s^26p^65f^2 \qquad (12)$$

(ASF with **3** CSFs in jj coupling),

$$\mathrm{AS}_6 = \mathrm{AS}_0+\{6d,6f\} \qquad (13)$$

(ASF with **12** CSFs in jj coupling),

$$\mathrm{AS}_7 = \mathrm{AS}_6+\{7s,7p,7d,7f\} \qquad (14)$$

(ASF with **37** CSFs in jj coupling),

$$\mathrm{AS}_8 = \mathrm{AS}_7+\{8s,8p,8d,8f\} \qquad (15)$$

(ASF with **75** CSFs in jj coupling),

$$\mathrm{AS}_9 = \mathrm{AS}_8+\{9s,9p,9d,9f\} \qquad (16)$$

(ASF with **126** CSFs in jj coupling),

$$\mathrm{AS}_{10} = \mathrm{AS}_9+\{10s,10p,10d,10f\} \qquad (17)$$

(ASF with **190** CSFs in jj coupling).

Table 1. The largest weights c_i (1) for the lowest energy ASF of U^{4+} ions in jj coupling calculated using the following ASs of orbitals: $AS_{0'}$, AS_0, AS_6, AS_7, AS_8, AS_9, AS_{10}. The field was formed by 50 nearest neighbours.

Configurations	$AS_{0'}$	AS_0	AS_6	AS_7	AS_8	AS_9	AS_{10}
$5f^2_-\quad J=4$	1.0	0.974	0.977	0.978	0.978	0.978	0.978
$5f^1_-\ J_1=\frac{5}{2}\quad 5f^1_+\ J_2=\frac{7}{2}\quad J=4$	0.0	0.217	0.206	0.200	0.199	0.199	0.199

Table 2. The largest weights b_r (3) for the lowest energy ASF of U^{4+} ions in LS coupling (transformed from the jj coupling results, see (3)). Here w and ν are the parameters of irreducible representations of the $R(7)$ and $G(2)$ groups.

Configurations	$AS_{0'}$	AS_0	AS_6	AS_7	AS_8	AS_9	AS_{10}
$5f^2, (w=1)\nu=2, {}^3H_4$	0.865	0.944	0.941	0.939	0.939	0.939	0.939
$5f^2, (w=1)\nu=2, {}^1G_4$	0.474	0.323	0.331	0.336	0.336	0.336	0.336
$5f^2, (w=1)\nu=2, {}^3F_4$	−0.165	−0.028	−0.035	−0.039	−0.039	−0.039	−0.039

At all steps only new orbitals were optimized and the initial shape of the radial orbitals in the multiconfiguration Dirac–Fock equations were obtained in the Thomas–Fermi potential. The weights c_i of the most relevant CSFs in the multiconfiguration expansion for the lowest atomic state function $J=4$ of U^{4+} ions are given in Table 1. The results have been used to transform this ASF from jj to LS coupling scheme, with the help of transformation matrices. The results of such transformation are presented in Table 2 and show that the ground state of U^{4+} ions in LS coupling is in agreement with Hund's rules.

The calculated CF energy levels for U^{4+} ion in MCDF+B+QED approach with valence–valence (VV) correlations are presented in Table 3. Calculations have been performed both taking into account the J-mixing and neglecting it. In the former case, the wavefunctions of the CF sub-levels are defined by (9), and all types of active set of orbitals (11)–(17) were used. In the second case the wavefunctions of the CF sub-levels are defined by (10). We included in this case the lowest three ASFs for each $J=0,\ldots,6$ values. The ASFs were constructed with 102 CSFs for $J=0$, 189 CSFs for $J=1$, 271 CSFs for $J=2$, 233 CSFs for $J=3$, 190 CSFs for $J=4$, 100 CSFs for $J=5$, and 57 CSFs for $J=6$ when the restricted active spaces of the CSFs were generated using AS_{10} active set of orbitals.

Table 4 presents the main weights c_{ia} (see (9)) for the lowest eigenfunctions of U^{4+} ion in MCDF+B+QED with VV correlations. The field was formed by 50 nearest neighbours.

The CF energy splittings calculated under various approximations, and including different numbers of closest-neighbour ligands, are reported in Table 5. Calculations were performed with the MCDF method

Table 3. Crystal-field energy levels for U^{4+} ions in MCDF+B+QED approximation with VV correlations, without and with J mixing. The field was formed with 98 ions.

States	CF energy levels in meV					
	AS_0	AS_6	AS_7	AS_8	AS_9	AS_{10}
	Calculated without J mixing					
Γ_5	0.0	0.0	0.0	0.0	0.0	0.0
	0.0	0.0	0.0	0.0	0.0	0.0
	0.0	0.0	0.0	0.0	0.0	0.0
Γ_3	139.2	140.0	137.5	138.1	137.9	138.2
	139.2	140.0	137.5	138.1	137.9	138.2
Γ_4	154.4	156.5	154.0	154.6	154.4	154.7
	154.4	156.5	154.0	154.6	154.4	154.7
	154.5	156.6	154.0	154.6	154.5	154.7
Γ_1	175.8	179.7	177.1	177.8	177.6	177.8
	Calculated with J mixing					
Γ_5	0.0	0.0	0.0	0.0	0.0	0.0
	0.0	0.0	0.0	0.0	0.0	0.0
	0.0	0.0	0.0	0.0	0.0	0.0
Γ_3	156.6	156.6	154.3	155.0	154.8	155.2
	156.6	156.6	154.3	155.0	154.9	155.2
Γ_4	152.3	162.1	159.8	160.5	160.3	160.7
	152.3	162.1	159.8	160.5	160.3	160.7
	152.3	162.1	159.8	160.6	160.4	160.7
Γ_1	186.5	189.8	187.7	188.6	188.5	188.9

(Coulomb section of Table 5), and with the RCI method, including Coulomb and transverse Breit interactions (+BREIT section of Table 5), and including Coulomb, transverse Breit, and QED effects (+QED section of Table 5). It appears that the latter do not influence in this case the energy spectrum, and that the MCDF *ab initio* values obtained with 96 ligands are in good agreement with experimental results based on high-resolution inelastic neutron scattering [4, 14].

Table 4. The largest weights c_{ia} (see (9)) for the lowest energy eigenfunctions of U^{4+} ions in MCDF+B+QED with VV correlations. The field was formed by 50 nearest neighbours.

States	$M_J=-4$	$M_J=-3$	$M_J=-2$	$M_J=-1$	$M_J=0$	$M_J=1$	$M_J=2$	$M_J=3$	$M_J=4$
Γ_5	0.000	**0.787**	0.123	0.181	0.000	0.297	0.123	0.479	0.000
	0.000	0.092	**0.693**	0.060	0.000	0.035	**0.693**	0.159	0.000
	0.000	0.470	0.074	0.305	0.000	0.178	0.074	**0.808**	0.000
Γ_3	0.540	0.000	0.005	0.000	**0.646**	0.000	0.005	0.000	0.540
	0.003	0.000	**0.707**	0.000	0.004	0.000	**0.707**	0.000	0.003
Γ_4	**0.707**	0.007	0.000	0.018	0.000	0.018	0.000	0.007	**0.707**
	0.020	0.249	0.000	**0.663**	0.000	**0.660**	0.000	0.250	0.020
	0.004	0.205	0.000	**0.784**	0.000	0.543	0.000	0.296	0.004
Γ_1	0.457	0.000	0.000	0.000	**0.763**	0.000	0.000	0.000	0.457

Table 5. Crystal-field energy levels for U^{4+} ions with VV correlations in AS_{10} and different types of interactions in the RCI approach. J-mixing effects are included. The field was formed by 8, 20, 44, 50, 74, and 98 ions.

States	CF energy levels in meV						
	8	20	44	50	74	98	Exp. [4, 14]
				Coulomb (MCDF)			
Γ_5	0.0	0.0	0.0	0.0	0.0	0.0	
	0.0	0.0	0.0	0.0	0.0	0.0	
	0.0	0.0	0.0	0.0	0.0	0.0	
Γ_3	167.8	156.5	151.0	156.0	158.4	156.5	
	167.8	156.5	151.0	156.0	158.4	156.5	
Γ_4	180.0	166.3	160.0	165.7	168.4	166.3	
	180.0	166.3	160.0	165.7	168.4	166.3	
	180.0	166.3	160.1	165.8	168.5	166.4	
Γ_1	204.4	181.9	173.5	181.2	184.9	182.1	
				+BREIT			
Γ_5	0.0	0.0	0.0	0.0	0.0	0.0	
	0.0	0.0	0.0	0.0	0.0	0.0	
	0.0	0.0	0.0	0.0	0.0	0.0	
Γ_3	165.5	155.2	149.9	154.8	157.1	155.2	
	165.5	155.2	150.0	154.8	157.1	155.3	
Γ_4	174.1	160.6	154.6	160.1	162.7	160.7	
	174.1	160.6	154.6	160.1	162.7	160.7	
	174.1	160.6	154.6	160.1	162.7	160.7	
Γ_1	210.7	188.7	180.2	188.0	191.7	188.9	
				+QED			
Γ_5	0.0	0.0	0.0	0.0	0.0	0.0	0.0
	0.0	0.0	0.0	0.0	0.0	0.0	0.0
	0.0	0.0	0.0	0.0	0.0	0.0	0.0
Γ_3	165.5	155.2	145.0	154.7	157.0	155.2	150.1
	165.5	155.2	145.0	154.8	157.1	155.2	150.1
Γ_4	174.1	160.6	154.6	160.1	162.7	160.7	166.7
	174.1	160.6	154.6	160.1	162.7	160.7	166.7
	174.1	160.6	154.6	160.1	162.7	160.7	166.7
Γ_1	210.7	188.7	180.2	188.0	191.7	188.9	174.8

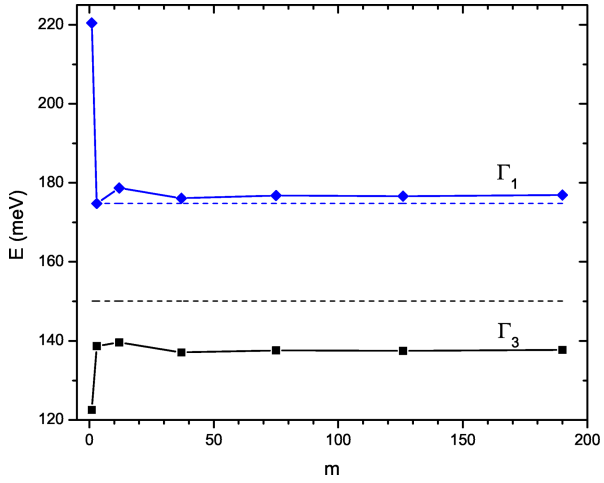

Fig. 1. Dependence of the CF energy levels of U^{4+} ions on the size of the MCDF space (the parameter m) without J mixing. The field was formed by 50 ions. The dashed lines indicate experimental values.

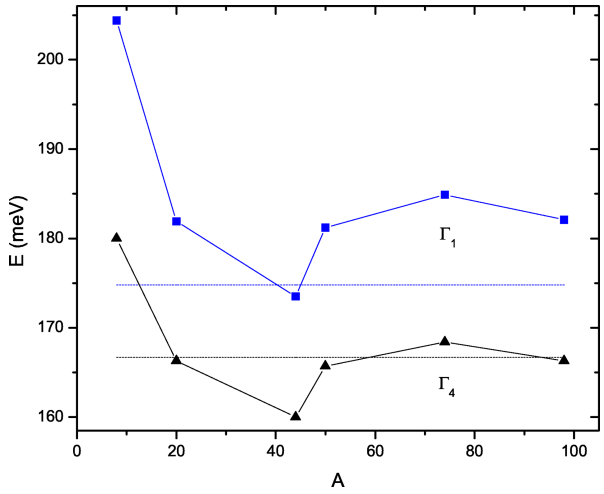

Fig. 2. Dependence of the CF energy of U^{4+} ions on the number of ligands (the parameter A) in the MCDF approach including J mixing effects. The dotted lines indicate experimental values.

The dependence of the CF energy on the calculation approach, on the size of the MCDF space, and on the number of ligand ions is also presented in Table 3, as well as in Table 5, Fig. 1 and Fig. 2. It appears that the energy of the Γ_1 and Γ_2 levels does not depend significantly on the size of the ASF space, whereas the number of ligands taken into account is much more important. Therefore, for an accurate determination of the CF energy levels in uranium dioxide, one must consider as many neighbours as practically possible, and then take into consideration the main contributions of correlation and relativistic effects.

In order to estimate the uncertainties in the calculated values of the CF energy of U^{4+} ion, their accuracy, and the role of correlation and relativistic effects, we have calculated the root-mean-square (rms) deviations of the calculated results from the available experimental data [4, 14]:

$$\sigma_M = \sqrt{\frac{\sum_{i=1}^{M}\left[\Delta E_{\text{exp}}\left(\Gamma_i\right) - \Delta E_{\text{the}}\left(\Gamma_i\right)\right]^2}{M}} \tag{18}$$

and

$$\sigma_J = \sqrt{\frac{\sum_{i=1}^{M}\left[\Delta E_{\text{exp}}(\Gamma_i) - \Delta E_{\text{the}}(\Gamma_i)\right]^2 D_{\Gamma_i}}{\sum_{i=1}^{M} D_{\Gamma_i}}}, \tag{19}$$

where $M = 4$ in (18) and D_{Γ_i} in (19) is the degeneracy of the states Γ_5, Γ_3, Γ_4, and Γ_1. The resulting rms deviation values are:

$$\sigma_M = 8.58, \quad \sigma_J = 8.97 \tag{20}$$

for MCDF+B+QED, AS_{10}, without J-mixing, $A = 98$,

$$\sigma_M = 8.07, \quad \sigma_J = 6.31 \tag{21}$$

for MCDF+B+QED, AS_{10}, with J-mixing, $A = 98$,

$$\sigma_M = 4.86, \quad \sigma_J = 3.88 \tag{22}$$

for MCDF, AS_{10}, with J-mixing, $A = 98$.

These values indicate that slightly better are the results obtained in the framework of the Dirac–Fock method in which transverse Breit interaction and the QED corrections are omitted.

Table 6. Crystal-field energy levels for Np^{4+} ions in NpO_2 calculated in MCDF+B+QED approximation with VV correlations AS_{10} (the best approach). The field was formed by 8, 20, 44, 50, 74, 98 ligand ions.

States	CF energy levels in meV					
	8	20	44	50	74	98
Γ_8	0.0	0.0	0.0	0.0	0.0	0.0
	0.0	0.0	0.0	0.0	0.0	0.0
	0.0	0.0	0.0	0.0	0.0	0.0
	0.0	0.0	0.0	0.0	0.0	0.0
Γ_8	37.9	32.6	31.0	32.5	33.2	32.7
	37.9	32.6	31.0	32.5	33.2	32.7
	37.9	32.6	31.0	32.5	33.2	32.7
	37.9	32.6	31.0	32.5	33.2	32.7
Γ_6	108.1	103.6	100.9	103.3	104.5	103.6
	108.1	103.6	100.9	103.3	104.5	103.6

Table 7. Crystal-field energy levels for Np^{4+} ions in MCDF+B+QED approach with VV correlations using the following ASs of orbitals: $AS_{0'}$, AS_0, AS_6, AS_7, AS_8, AS_9, and AS_{10}. The field was formed by 98 ligand ions.

States	CF energy levels in meV								
	Calculated without J mixing							J mix.	Exp. [16]
	$AS_{0'}$	AS_0	AS_6	AS_7	AS_8	AS_9	AS_{10}	AS_{10}	
Γ_8	0.0	0.0	0.0	0.0	0.0	0.0	0.0	0.0	0.0
	0.0	0.0	0.0	0.0	0.0	0.0	0.0	0.0	0.0
	0.0	0.0	0.0	0.0	0.0	0.0	0.0	0.0	0.0
	0.0	0.0	0.0	0.0	0.0	0.0	0.0	0.0	0.0
Γ_8	1.1	32.4	32.7	32.3	32.5	32.6	32.7	33.7	55
	1.1	32.4	32.7	32.3	32.5	32.6	32.7	33.7	55
	1.1	32.4	32.7	32.4	32.5	32.6	32.7	33.7	55
	1.1	32.4	32.7	32.4	32.5	32.6	32.7	33.7	55
Γ_6	2.2	102.9	103.3	102.4	103.1	103.2	103.6	99.2	270
	2.2	102.9	103.3	102.4	103.1	103.2	103.6	99.2	270

4. Calculations of the crystal-field splitting of the ground state of Np^{4+} ions in NpO_2

In the paramagnetic phase of NpO_2 the ten times degenerate $J = 9/2$ multiplet splits into three sub-levels, namely two Γ_8 quartets and one Γ_6 doublet [15].

For the generation of CSFs for the ground state of the free Np^{4+} ion we used the following approach. The configuration state functions of the multiconfiguration calculations include single and double substitutions from the valence 5f shell (VV correlation). Restricted active spaces (RAS) of the CSFs are generated using the following ASs of the orbitals:

$$AS_{0'} = 1s^2 2s^2 2p^6 3s^2 3p^6 3d^{10} 4s^2 4p^6 4d^{10} 4f^{14} \; 5s^2 5p^6 5d^{10} 6s^2 6p^6 5f^3 \quad (23)$$

(ASF with **1** CSFs in jj coupling),

$$AS_0 = 1s^2 2s^2 2p^6 3s^2 3p^6 3d^{10} 4s^2 4p^6 4d^{10} 4f^{14} \; 5s^2 5p^6 5d^{10} 6s^2 6p^6 5f^3 \quad (24)$$

(ASF with **7** CSFs in jj coupling),

$$AS_6 = AS_0 + \{6d, 6f\} \quad (25)$$

(ASF with **62** CSFs in jj coupling),

$$AS_7 = AS_6 + \{7s, 7p, 7d, 7f\} \quad (26)$$

(ASF with **265** CSFs in jj coupling),

$$AS_8 = AS_7 + \{8s, 8p, 8d, 8f\} \quad (27)$$

(ASF with **613** CSFs in jj coupling),

$$AS_9 = AS_8 + \{9s, 9p, 9d, 9f\} \quad (28)$$

(ASF with **1106** CSFs in jj coupling),

$$AS_{10} = AS_9 + \{10s, 10p, 10d, 10f\} \quad (29)$$

(ASF with **1744** CSFs in jj coupling).

The calculated CF energy levels in MCDF+B+QED approach with VV correlations are reported in Tables 6 and 7. Table 6 shows the dependence of the CF splitting on the number of ligand ions. Table 7 shows the dependence on the correlation effects (multiconfiguration expansion).

Table 7 gives the results of final calculations considering 98 ligand ions. Calculations are performed both with and without J-mixing. We included the lowest three ASFs for each $J = 1/2, \ldots, 13/2$ values in the J-mixing calculations, totally 21 ASFs. The ASFs were constructed with 853 CSFs for $J = 1/2$, 1543 CSFs for $J = 3/2$, 1947 CSFs for $J = 5/2$, 2007 CSFs for $J = 7/2$, 1744 CSFs for $J = 9/2$, 1314 CSFs for $J = 11/2$, and 844 CSFs for $J = 13/2$.

The weights c_i of the most important configuration state functions (CSFs) in the multiconfiguration expansion for the lowest atomic state function (ASF) $J = 9/2$ of the Np^{4+} ion are presented in Table 8. Using these results we transformed this ASF from the jj to the LS coupling scheme with the transformation matrices. The results of the transformation, presented in Table 9, show

Table 8. The largest weights c_i for the lowest energy ASF of Np^{4+} ion in jj coupling calculated using the following ASs of orbitals: $AS_{0'}$, AS_0, AS_6, AS_7, AS_8, AS_9, AS_{10}. The field was formed by 98 ligand ions.

Configurations	$AS_{0'}$	AS_0	AS_6	AS_7	AS_8	AS_9	AS_{10}
$5f^3_-\quad J=\frac{9}{2}$	1.000	0.875	0.882	0.885	0.885	0.885	0.885
$5f^2_-\ J_1=4\quad 5f^1_+\ J_2=\frac{7}{2}\quad J=\frac{9}{2}$		−0.443	−0.4318	−0.428	−0.427	−0.427	−0.427
$5f^1_-\ J_1=\frac{5}{2}\quad 5f^2_+\ J_2=2\quad J=\frac{9}{2}$		−0.126	−0.120	−0.118	−0.117	−0.117	−0.117
$5f^1_-\ J_1=\frac{5}{2}\quad 5f^2_+\ J_2=4\quad J=\frac{9}{2}$		0.116	0.110	0.108	0.108	0.108	0.108

Table 9. The largest weights b_r (3) for the lowest energy ASF of a Np^{4+} ion in LS coupling (transformed from the jj coupling results) calculated using the following ASs of orbitals: $AS_{0'}$, AS_0, AS_6, AS_7, AS_8, AS_9, AS_{10}. The field was formed by 98 ligand ions.

Configurations	$AS_{0'}$	AS_0	AS_6	AS_7	AS_8	AS_9	AS_{10}
$5f^3, (w=1)\nu=3, {}^4I_{9/2}$	**−0.674**	**−0.923**	**−0.918**	**−0.916**	**−0.916**	**−0.916**	**−0.915**
$5f^3, (w=2)\nu=3, {}^2H_{9/2}$	0.624	0.314	0.327	0.332	0.332	0.333	0.333
$5f^3, (w=1)\nu=3, 2H_{9/2}$	−0.146	−0.168	−0.169	−0.168	−0.168	−0.1685	−0.168
$5f^3, (w=1)\nu=3, {}^2G_{9/2}$	−0.203	−0.093	−0.097	−0.098	−0.098	−0.098	−0.098
$5f^3, (w=1)\nu=3, {}^4G_{9/2}$	−0.162	−0.046	−0.047	−0.048	−0.048	−0.048	−0.048
$5f^3, (w=1)\nu=3, {}^4F_{9/2}$	0.093	0.037	0.040	0.037	0.037	0.037	0.037
$5f^3, (w=2)\nu=3, {}^2G_{9/2}$	0.242	0.009	0.016	0.018	0.018	0.019	0.018

Table 10. Crystal-field energy levels for the Pu^{4+} ions in PuO_2 calculated in MCDF approximation, with VV correlations AS_9. The field was formed by the 8, 20, 44, and 50 ligand ions.

States	CF energy level in meV			
	8	20	44	50
Γ_1	0.0	0.0	0.0	0.0
Γ_4	54.76	54.51	53.53	54.41
	54.77	54.52	53.53	54.43
	54.77	54.52	53.53	54.43
Γ_3	93.89	93.46	91.78	93.30
	93.89	93.46	91.78	93.30
Γ_5	126.28	117.62	113.64	117.27
	126.28	117.62	113.64	117.27
	126.29	117.63	113.64	117.27

that the ground state of the Np^{4+} ion in the LS coupling is $^4I_{9/2}$, in agreement with Hund's rules.

5. Calculations of the crystal-field splitting of the ground state of Pu^{4+} ions in PuO_2

In the paramagnetic phase of PuO_2 the ninefold degenerate $J=4$ multiplet splits into four sub-levels: a Γ_1 singlet, a Γ_3 doublet, and two triplets, Γ_4 and Γ_5 [15, 17].

For the generation of CSFs for the ground state of the free Pu^{4+} ion we also used the configuration state functions of the multiconfigurational calculations including single and double substitutions from the valence 5f shell (VV correlation). Restricted active spaces (RAS) of the CSFs were generated using the following ASs of orbitals:

$$\begin{aligned} AS_{0'} = {} & 1s^2 2s^2 2p^6 3s^2 3p^6 3d^{10} 4s^2 4p^6 4d^{10} 4f^{14} \\ & 5s^2 5p^6 5d^{10} 6s^2 6p^6 5f^4 \\ & (\text{ASF with } \mathbf{1} \text{ CSFs in } jj \text{ coupling}), \end{aligned} \tag{30}$$

$$\begin{aligned} AS_0 = {} & 1s^2 2s^2 2p^6 3s^2 3p^6 3d^{10} 4s^2 4p^6 4d^{10} 4f^{14} \\ & 5s^2 5p^6 5d^{10} 6s^2 6p^6 5f^4 \\ & (\text{ASF with } \mathbf{19} \text{ CSFs in } jj \text{ coupling}), \end{aligned} \tag{31}$$

$$\begin{aligned} AS_6 = {} & AS_0 + \{6d, 6f\} \\ & (\text{ASF with } \mathbf{294} \text{ CSFs in } jj \text{ coupling}), \end{aligned} \tag{32}$$

$$\begin{aligned} AS_7 = {} & AS_6 + \{7s, 7p, 7d, 7f\} \\ & (\text{ASF with } \mathbf{1376} \text{ CSFs in } jj \text{ coupling}), \end{aligned} \tag{33}$$

$$\begin{aligned} AS_8 = {} & AS_7 + \{8s, 8p, 8d, 8f\} \\ & (\text{ASF with } \mathbf{3266} \text{ CSFs in } jj \text{ coupling}), \end{aligned} \tag{34}$$

$$\begin{aligned} AS_9 = {} & AS_8 + \{9s, 9p, 9d, 9f\} \\ & (\text{ASF with } \mathbf{5964} \text{ CSFs in } jj \text{ coupling}), \end{aligned} \tag{35}$$

Table 11. Crystal-field energy levels for the Pu^{4+} ions in PuO_2, calculated in MCDF approach with VV correlations using the following ASs of orbitals: $AS_{0'}$, AS_0, AS_6, AS_7, AS_8, AS_9, and AS_{10}. The field was formed by 50 ligand ions.

States	CF energy levels in meV									
	Calculated without J mixing							J mix.	LDA [17]	Exp. [18]
	$AS_{0'}$	AS_0	AS_6	AS_7	AS_8	AS_9	AS_{10}	AS_{10}		
Γ_1	0.0	0.0	0.0	0.0	0.0	0.0	0.0	0.0	0.0	0.0
Γ_4	44.13	51.60	52.53	53.76	54.12	54.41	54.52	64.25	99	123
	44.16	51.62	52.54	53.77	54.13	54.43	54.53	64.25	99	123
	44.16	51.62	52.54	53.77	54.13	54.43	54.53	64.25	99	123
Γ_3	75.69	88.47	90.06	92.17	92.79	93.30	93.47	102.81	162	
	75.69	88.48	90.07	92.18	92.79	93.30	93.48	102.82	162	
Γ_5	169.65	107.03	111.20	115.44	116.47	117.27	117.53	127.00	208	
	169.65	107.03	111.20	115.44	116.47	117.27	117.53	127.00	208	
	169.65	107.04	111.21	115.45	116.47	117.27	117.54	127.01	208	

Table 12. Crystal-field energy levels for Am^{4+} ion in AmO_2 calculated in MCDF approximation, with VV correlations, using the following ASs of orbitals: AS_0, AS_6, AS_7, and AS_8. The field was formed by 50 ligand ions.

States	CF energy levels in meV			
	AS_0	AS_6	AS_7	AS_8
Γ_8	0.00	0.00	0.00	0.00
	0.00	0.00	0.00	0.00
	0.03	0.03	0.03	0.03
	0.03	0.03	0.03	0.03
Γ_7	13.95	9.26	5.69	5.31
	13.95	9.26	5.69	5.31

$$AS_{10} = AS_9 + \{10s, 10p, 10d, 10f\} \tag{36}$$

(ASF with **9470** CSFs in jj coupling).

The calculated CF energy levels for the Pu^{4+} ions in MCDF approach with VV correlations are presented in Tables 10 and 11. Table 10 illustrates the dependence of the CF splitting on the number of ligand ions, whereas Table 11 shows the dependence on the correlation effects (multiconfiguration expansion). It follows that the ground state of the Pu^{4+} ions in LS coupling is $^5I_4$, in agreement with Hund's rules.

In Table 11 we give the results of final calculations including 50 ligands. They are compared with the theoretical calculation based on the local density approximation (LDA) to density-functional theory [17] and experimental data [18]. Our calculations were performed both with and without J-mixing. For the J-mixing calculations we used the restricted active space of the CSFs generated by the AS_{10} active set of orbitals (17). We included in this case the lowest three ASFs for each of $J = 0, \ldots, 6$ values. The ASFs were constructed with 1976 CSFs for $J = 0$, 5295 CSFs for $J = 1$, 8021 CSFs for $J = 2$, 9237 CSFs for $J = 3$, 9470 CSFs for $J = 4$, 8411 CSFs for $J = 5$, and 6877 CSFs for $J = 6$.

6. Calculations of the crystal-field splitting of the ground state of Am^{4+} ion in AmO_2

In the paramagnetic phase of AmO_2 the six times degenerate $J = 5/2$ multiplet splits into two sub-levels, namely a Γ_8 quartet and a Γ_7 doublet [19, 15].

For the generation of CSFs for the ground state of the free Am^{4+} ion we used the configuration state functions of the multiconfiguration calculations including the single and double substitutions from the valence 5f shell (VV correlation). Restricted active spaces (RAS) of the CSFs have been generated using the following ASs of the orbitals:

$$AS_0 = 1s^2 2s^2 2p^6 3s^2 3p^6 3d^{10} 4s^2 4p^6 4d^{10} 4f^{14} \\ 5s^2 5p^6 5d^{10} 6s^2 6p^6 5f^5 \tag{37}$$

(ASF with **28** CSFs in jj coupling),

$$AS_6 = AS_0 + \{6d, 6f\} \tag{38}$$

(ASF with **756** CSFs in jj coupling),

$$AS_7 = AS_6 + \{7s, 7p, 7d, 7f\} \tag{39}$$

(ASF with **3847** CSFs in jj coupling),

$$AS_8 = AS_7 + \{8s, 8p, 8d, 8f\} \tag{40}$$

(ASF with **9358** CSFs in jj coupling).

Table 13. Crystal-field energy levels for the Am^{4+} ions in AmO_2 calculated in MCDF+B+QED approximation, with VV correlations, using the following ASs of orbitals: AS_0, AS_6, AS_7, and AS_8. The field was formed by the 50 ligand ions. We note that the available experimental results indicate the Γ_7 doublet, and not the Γ_8 quartet, as the ground state.

States	CF energy levels in meV					
	Calculated without J mixing				J mix.	Exp. [19]
	AS_0	AS_6	AS_7	AS_8	AS_8	
Γ_8	0.00	0.00	0.00	0.00	0.0	0.0
	0.00	0.00	0.00	0.00	0.0	0.0
	0.03	0.03	0.03	0.03	0.3	0.0
	0.03	0.03	0.03	0.03	0.3	0.0
Γ_7	16.85	12.20	8.93	8.52	10.74	-4.34
	16.85	12.20	8.93	8.52	10.74	-4.34

The calculated CF energy levels for the Am^{4+} ion in MCDF and MCDF+B+QED approximations, with VV correlations, are presented in Tables 12 and 13 respectively. The results obtained show that the ground state of the Am^{4+} ion in LS coupling is $^6H_{5/2}$, in agreement with Hund's rules.

Table 13 gives the results of final calculations including 50 ligands. Calculations have been performed both with and without J-mixing. We included in the first case the lowest three ASFs for each $J = 1/2, \ldots, 13/2$ values. The ASFs were constructed with 3791 CSFs for $J = 1/2$, 7068 CSFs for $J = 3/2$, 9358 CSFs for $J = 5/2$, 10471 CSFs for $J = 7/2$, 10406 CSFs for $J = 9/2$, 9391 CSFs for $J = 11/2$, and 7740 CSFs for $J = 13/2$.

It must be noticed that, in the case of AmO_2, a serious disagreement with experimental data apparently occurs, as Karraker [19] has indicated the Γ_7 doublet and not the Γ_8 quartet as the ground state. However, the available data do not seem to be conclusive for a number of reasons, and the need for more experimental investigations of this material has been pointed out [4].

7. Conclusions

The results reported in this paper illustrate the high efficiency of the extended GRASP2K [12, 13] package for calculations of the crystal-field energy levels in ionic solids. The version of the package is based on the generalized multiconfiguration Dirac–Fock method for large-scale *ab initio* calculations of the crystal-field energy levels.

The calculated energy spectrum of the U^{4+} ion in the paramagnetic phase of uranium dioxide is in very good agreement with the results of neutron spectroscopy experiments. However, the agreement between calculations and experimental data becomes worse with increasing atomic weight, to the point that the wrong CF ground state is predicted for AmO_2. Possible explanations of this behaviour may be the changes in the nature of crystal-field effects (resulting for example from the large, unexpected orbital mixing suggested by Prodan et al. [20]) and point to the necessity of further refinements to the present theory.

Comparing the relative roles of the correlation effects and the number of neighbour ions we arrive at the conclusion that it is important first to take into account as many ligand ions as practically possible and only then to take into consideration the main contributions of correlations and relativistic effects. Unfortunately, the convergency of the process taking account of correlation effects is rather slow.

References

[1] Z. Rudzikas, *Theoretical Atomic Spectroscopy* (Cambridge University Press, 1997, 2nd ed. 2007).
[2] G. Gaigalas, E. Gaidamauskas, Z. Rudzikas, N. Magnani, and R. Caciuffo, Phys. Rev. A **79**, 022511 (2009).
[3] M.T. Hutchings, in: *Solid State Physics*, vol. 16, eds. F. Seitz and D. Turnbull (Academic Press, New York, 1964) p. 227.
[4] P. Santini, S. Carretta, G. Amoretti, R. Caciuffo, N. Magnani, and G.H. Lander, Rev. Mod. Phys. **81**, 807 (2009).
[5] S.B. Wilkins, R. Caciuffo, C. Detlefs, J. Rebizant, E. Colineau, F. Wastin, and G.H. Lander, Phys. Rev. B **73**, 060406 (2006).
[6] N. Magnani, S. Carretta, R. Caciuffo, P. Santini, G. Amoretti, A. Hiess, J. Rebizant, and G.H. Lander, Phys. Rev. B **78**, 104425 (2008).
[7] P. Santini, S. Carretta, N. Magnani, G. Amoretti, and R. Caciuffo, Phys. Rev. Lett. **97**, 207203 (2006).
[8] J. Narušis and J. Batarūnas, Liet. Fiz. Rink. **10**, 718 (1970) [in Russian].
[9] G. Gaigalas, T. Zalandauskas, and Z. Rudzikas, At. Data Nucl. Data Tables **84**, 99 (2003).
[10] G. Gaigalas, S. Fritzsche, and I.P. Grant, Comput. Phys. Commun. **139**, 263 (2001).
[11] K.G. Dayall, I.P. Grant, C.T. Johnson, F.A. Parpia, and E.P. Plummer, Comput. Phys. Commun. **55**, 425 (1989).
[12] C. Froese Fischer, G. Gaigalas, and Y. Ralchenko, Comput. Phys. Commun. **175**, 738 (2006).
[13] P. Jönsson, X. He, C. Froese Fischer, and I.P. Grant, Comput. Phys. Commun. **177**, 597 (2007).

[14] G. Amoretti A. Blaise, R. Caciuffo, J.M. Fournier, M.T. Hutchings, R. Osborn, and A.D. Taylor, Phys. Rev. B **40**, 1856 (1989).
[15] N. Magnani, P. Santini, G. Amoretti, and R. Caciuffo, Phys. Rev. B **71**, 054405 (2005).
[16] G. Amoretti, A. Blaise, R. Caciuffo, D. Di Cola, J.M. Fournier, M.T. Hutchings, G.H. Lander, R. Osborn, A. Severing, and A.D. Taylor, J. Phys. Condens. Matter **4**, 3459 (1992).
[17] M. Colarieti-Tosti, O. Eriksson, L. Nordström, J. Wills, and M.S.S. Brooks, Phys. Rev. B **65**, 195102 (2002).
[18] S. Kern, R.A. Robinson, H. Nakotte, G.H. Lander, B. Cort, P. Watson, and F.A. Vigil, Phys. Rev. B **59**, 104 (1999).
[19] D.G. Karraker, J. Chem. Phys. **63**, 3174 (1975).
[20] I.D. Prodan, G.E. Scuseria, and R.L. Martin, Phys. Rev. B **76**, 033101 (2007).

KRISTALINIO LAUKO AKTINIDŲ DIOKSIDUOSE *AB INITIO* SKAIČIAVIMAI

G. Gaigalas[a], E. Gaidamauskas[a], Z. Rudzikas[a], N. Magnani[b], R. Caciuffo[b]

[a] *Vilniaus universiteto Teorinės fizikos ir astronomijos institutas, Vilnius, Lietuva*
[b] *Europos Komisija, Jungtinis Tyrimų Centras, Transuraninių elementų institutas, Karlsruhe, Vokietija*

Santrauka

Sunkiųjų cheminių elementų spektroskopinių tyrimų svarba nuolat didėja. Tačiau tokių elementų fizika yra labai sudėtinga, čia būtina derinti precizinius eksperimentus su kaip galima tikslesniais teoriniais tyrimais.

Darbas skirtas įvertinti koreliacinių, reliatyvistinių ir radiacinių efektų įtaką aktinidų dioksidų spektrinėms charakteristikoms. Tiriami urano, neptūnio, plutonio ir americio oksidų energijų spektrai. Taikomi daugiakonfigūracinis Dirako ir Foko bei reliatyvistinis konfigūracijų superpozicijos artiniai bei atsižvelgiama į aukštesnių eilių reliatyvistines ir radiacines pataisas.

Gautieji rezultatai liudija aukštą taikomų metodų tikslumą ir efektyvumą. Kartu pabrėžiama būtinybė visų pirma atsižvelgti į kuo didesnį urano atomą supančių jonų kiekį, o tik po to – kuo tiksliau į koreliacinius ir reliatyvistinius efektus.